Regulation of the cognitive aging process by the transcriptional repressor RP58

Tomoko Tanaka[1], Shinobu Hirai[2], Hiroyuki Manabe[3], Kentaro Endo[4], Hiroko Shimbo [2], Haruo Okado [2, *]

[1] Department of Basic Medical Science, Tokyo Metropolitan Institute of Medical Science, Tokyo, Japan.

[2] Department of Psychiatry & Behavioral Science, Tokyo Metropolitan Institute of Medical Science, Tokyo, Japan.

[3] Laboratory of Neural Information, Graduate School of Brain Science, Doshisha University, Kyoto, Japan.

[4] Center for Basic Technology Research, Tokyo Metropolitan Institute of Medical Science, Tokyo, Japan.

* Correspondence should be addressed to Haruo Okado, Department of Psychiatry & Behavioral Science, Tokyo Metropolitan Institute of Medical Science, Tokyo 156-8506, Japan. Tel: +81-3-6834-2403, Fax: +81-3-5316-3150, E-mail: okado-hr@igakuken.or.jp (H.O.)

Acknowledgments

The authors thank Dr. Makoto Hashimoto for advice. The authors thank Kazuki

Shiotani and Yuta Tanisumi for their contribution to help us with analysis of electrophysiology data. We would like to thank Editage (www.editage.com) for English language editing.

Funding

This work was partially supported by JSPS KAKENHI Grant Number 18H02537 for Haruo Okado, and by JSPS KAKENHI Grant Number 17K16408 and Research Grant for Public Health Science for Tomoko Tanaka.

Abstract

Aging involves a decline in physiology which is a natural event in all living organisms. An accumulation of DNA damage contributes to the progression of aging. DNA is continually damaged by exogenous sources and endogenous sources. If the DNA repair pathway operates normally, DNA damage is not life threatening. However, impairments of the DNA repair pathway may result in an accumulation of DNA damage, which has a harmful effect on health and causes an onset of pathology. RP58, a zinc-finger transcriptional repressor, plays a critical role in cerebral cortex formation. Recently, it has been reported that the expression level of RP58 decreases in the aged human cortex. Furthermore, the role of RP58 in DNA damage is inferred by the involvement of DNMT3, which acts as a co-repressor for RP58, in DNA damage. Therefore, RP58 may play a crucial role in the DNA damage associated with aging. In the present study, we investigated the role of RP58 in aging. We used RP58 hetero-knockout and wild-type mice in adolescence, adulthood, or old age. We performed immunohistochemistry to determine whether microglia and DNA damage markers responded to the decline in RP58 levels. Furthermore, we performed an object location test to measure cognitive function, which decline with age. We found that the wild-type mice showed an increase in single-stranded DNA and gamma-H2AX foci. These results indicate an increase in DNA damage

or dysfunction of DNA repair mechanisms in the hippocampus as age-related changes. Furthermore, we found that, with advancing age, both the wild-type and hetero-knockout mice showed an impairment of spatial memory for the object and increase in reactive microglia in the hippocampus. However, the RP58 hetero-knockout mice showed these symptoms earlier than the wild-type mice did. These results suggest that a decline in RP58 level may lead to the progression of aging.

Keyword: Aging, DNA damage, DNA repair, microglia, RP58

Introduction

In humans, cognitive and motor function develop in association with maturation, followed by decline in advancing age. Aging is an age-related decline in physiology which is a natural event in all living organisms. Aging is a risk factor for neurodegenerative disorders, cancer, and other chronic disorders. An accumulation of DNA damage contributes to the progression of aging. DNA is continually damaged by exogenous sources, including radiation, diet, environmental chemicals, and endogenous sources, which include spontaneous errors during DNA replication and reactive oxygen species. If DNA repair operates normally, DNA damage is not serious for daily life. On the other hand, the accumulation of DNA damage by the impairment of the DNA repair pathway and the increase in DNA damage has a harmful effect on postgrowth health and the onset of pathology [10, 18]. It has been demonstrated that abnormal microglia, which show hallmark features of priming, were detected in a DNA repair-deficient mouse model, which displays accelerated aging in multiple tissues, including the CNS [25]. Although the expression of primed microglia, which show an exaggerated and uncontrolled inflammatory response to an immune stimulus, becomes increasingly common with age [20, 24], the relationship between DNA damage, inflammation and aging remains unclear.

RP58, which has a zinc-finger transcriptional repressor at the C-terminus and BTB-domain at the N-terminus, is a transcriptional repressor [1]. Although RP58 plays a critical role in the formation of the cerebral cortex, its expression continues after maturation [21, 22]. Recently, it has been reported that the expression level of RP58 decreases in the aged human cortex by examining post-mortem brains [17]. Therefore, RP58 may be involved in aging. Furthermore, the role of RP58 in DNA damage with aging is inferred by the fact that DNA methyltransferase 3 (DNMT3), which acts as a co-repressor of RP58, is involved in DNA damage [7, 8]. However, the mechanism of how RP58 contributes to aging remains unclear.

We focused on the function of RP58 in DNA damage and repair, which are important for aging. We investigated whether RP58 plays an important role in the maintenance of cognitive function as an age-related phenomenon and the underlying mechanism. We clarified that wild-type mice showed the accumulation of DNA damage, an age-related changes, especially in mossy cells, which plays a role in encode spatial information and are located in the hilus of the hippocampus. Furthermore, we found that the wild-type mice showed an impairment of place memory for objects with advancing age.However, RP58 hetero-knockout mice ($RP58^{+/-}$ mice) showed these symptoms earlier than the wild-type mice did. Continuous treatment of minocycline, which has neuroprotective and anti-

inflammation effect [13, 31], prevented the above phenomenon. Therefore, it is suggested that a decline of RP58 level may lead to the progression of aging through the accumulation of DNA damage and abnormalities in microglia.

Materials and methods

All experimental procedures were approved by the Animal Experimentation Ethics Committee of the Tokyo Metropolitan Institute of Medical Science (49040).

Animals

The original lines of RP58 mutant mice ($RP58^{-/-}$) were established as a C57/BL6 congenic line (a genetic background strain) by repeated back-crosses, as described previously [23]. Because $RP58^{-/-}$mice are embryonically lethal, $RP58^{+/-}$ mice were chosen to investigate the process of aging. All mice were maintained under a 12:12 h light/dark cycle (lights on at 8:00 AM). All efforts were made to minimise the number of animals used and their suffering. All experiments were performed during adolescence (postnatal day 45 (P 45)-P60), adulthood (P90–P120), or old age (P365-P545).

Drug treatment

Minocycline was administered to the animals' drinking water from weaning to the day before the behavioral test or perfusion in the $RP58^{+/+}$ and the $RP58^{+/-}$ mice. Minocycline was dissolved in the filtrate water at 0.015 mg/ml.

Behavioral assessment

Male mice were allowed to habituate to the behavioral room for at least 1 hour before commencement of the behavioral test. Mice showing outlier behavior > 2 standard deviations or < 2 standard deviations from the mean were not analyzed as part of the behavioral test.

The object location test consisted of three phases. All phases were performed under a light intensity of 10 lux. On day 1, the animals were placed in an empty square box (50 cm x 50 cm) for 10 minutes. On day 2, the animals were placed in the same box for 10 minutes with two same identical unfamiliar objects. On day 3, the animals were placed in the same box, with one of the two items being displaced to a novel location in the area. The discrimination index was calculated as the ratio of the time spent exploring the novel place to that spent exploring the familiar place: discrimination index = (novel place exploration time – familiar place exploration time)/(novel place exploration time + familiar place exploration time). On each day, the exploration time in each place was calculated automatically using a DVTrack video tracking system (Muromachi, Tokyo, Japan).

Electrophysiology

Mice were anaesthetized with isoflurane (1.5%), and implanted with a custom-designed electrode comprising two tetrodes in the hippocampal CA1 (1.8 mm anterior to bregma, 1.4 mm lateral to the midline, and 1.2 mm from the brain surface). Individual tetrodes consisted of four twisted polyimide-coated tungsten wires (single wire diameter 12.7 μm; California Fine Wire, Grover Beach, CA). One additional screw was threaded into the bone above the cerebellum for reference and grounding. The electrodes were connected to an electrode interface board (EIB-18, Neuralynx, MT) on a microdrive. The behavioral assessment was performed at least 1 week after surgery.

Electrical signals were obtained with open-source hardware (Open Ephys, Cambridge, MA) during the object location test for local field potential (LFP) recording at a sampling rate of 30kHz. For synchronisation with behavioral data, a transistor-transistor logic (TTL) pulse was managed. After recording, electrode lesions were induced using 20 μ A direct current stimulation for 10 seconds using one of the four tetrode leads.

Analysis of electrophysiology data

All data analyses were performed using the built-in software in MATLAB (The MathWorks, Inc., MA, USA). LFPs were down-sampled to 1,000 Hz and the data were extracted 1 second before and after contact with the objects. Theta power was calculated

by taking the mean value of the power spectrum between 4-8 Hz. This value was normalized by theta power in which mice was on a walk.

Immunohistochemistry

In adolescence, adulthood or old age, male and female mice were anaesthetized with isoflurane and then sequentially perfused through the heart with PBS followed by 4% paraformaldehyde (PFA) in PBS. Their brains were post-fixed, cryoprotected in 20% sucrose overnight and 30% sucrose over 2 days at 4℃, and embedded in OCT compound and frozen. Coronal sections of mouse brains were then cut using a cryostat (20 μm). Free-floating sections containing the hippocampus were activated by HistVT one (Nakalai, Kyoto, Japan) at 70℃ for 20 minutes, incubated in 0.4% Block-ase (DS Pharma Biomedical., Osaka, Japan) in PBS at room temperature (RT) for 20 minutes, and then incubated with primary antibody (Supplemental figure 1). All primary antibodies were diluted 1:500 in PBS containing 0.3% Triton X-100. The sections were then incubated with secondary antibody (Jackson, Maine, United States) (diluted 1:500 in PBS containing 0.3% Triton X-100) for 2 hours at RT. All sections types were incubated with DAPI (Nacalai Tesque, Kyoto, Japan) for nuclear staining. Fluorescence micrographs of the sections subjected to immunostaining procedures were captured and

digitized using a FluoView® FV3000 confocal laser scanning microscope (Olympus, Tokyo, Japan).

Analysis of immunostaining images

To quantify single-stranded DNA (ssDNA) and gamma H2AX in the cells, the number of cells with five or more nuclear ssDNA foci or gamma H2AX foci was counted [16]. For activated microglia analysis, CD68 antibody staining were performed. CD68 is a lysosomal-associated protein in macrophages/microglia and is associated with phagocytic cells. The Iba1 antibody was used as a marker for both resting and activated microglia. Microglia with aggregated CD68 expression were categorised as reactive microglia, and the percentage of reactive microglia was compared between groups [2, 5].

X-ray

Animals were irradiated with a dose of 0.3 Gray. At 1 hour, 6hours or 24 hours after irradiation, mice were anaesthetized with isoflurane and then sequentially perfused through the heart with PBS followed by 4% PFA in PBS. Subsequent processes were the same way as those described in the immunohistochemistry section.

Electron microscopy

Tissue preparation: In adulthood, male and female mice were anaesthetized with isoflurane and then sequentially perfused through the heart with saline followed by 2% PFA and 2.5% glutaraldehyde in 0.1 mol/l PB (pH7.4). Their brains were post-fixed, and coronal sections of the mouse brain containing the dentate gyrus and prefrontal cortex were then cut using a VT1200S microslicer (300 μm) (Leica, Wetzlar, Germany). Micro-dissected areas were post-fixed at 4℃ for 2 hours in 2% osmium tetroxide in 0.1mol/l Cacodylate Buffer. Tissue blocks were dehydrated using 50% ethanol for 5 minutes, 70% ethanol for 15 minutes, 80% ethanol for 15 minutes, 90% ethanol for 15 minutes, 100% ethanol at RT for 20 minutes × 3, subsequently infiltrated with propylene oxide for 10 minutes × 3, 1:1 solution of propylene oxide: epoxy resin for 2 hours, and epoxy resin overnight. Each block was placed flat on glass microscope slides and horizontally mounted on gelatin capsules (Lilly, Indiana, USA). After embedding, each block was polymerized in epoxy resin (EPON 812, TAAB) (EMJapan, Tokyo, Japan) at 60°C for 48 hours. Polymerized blocks were trimmed to a section containing the dentate gyrus and prefrontal cortex using an ultramicrotome PowerTomeX (RMC Boeckeler, Arizona, USA). Semi-thin (1 μm) sections were stained with toluidine blue

and used to guide further cutting of the specimen block to ultra-thin sections (50-80 nm). Ultra-thin sections were placed in formvar-coated single-slot grids. After staining with uranyl acetate and lead citrate, ultra-thin sections were observed under a JEM-1400 transmission electron microscope (JEOL, Tokyo, Japan) equipped with a bottom-mounted CCD camera and subsequently processed using ImageJ.

Quantification of ultrastructural defects: Quantification of mitochondrial ultrastructural defects was performed from transmission electron microscopy images with a magnification of 10,000 ×. Images were taken 2 sections at least 10 sections within the tissue block in each region. Although mitochondria are sparse within astrocytic processes of the dentate gyrus, the criteria used by Siskova et al. [28] for the identification of astrocytes and neuronal cells were applied to ensure that predominantly, if not exclusively, neuronal mitochondria were included. Every mitochondria of neuronal origin were analysed and, based on their ultrastructural appearance, classified into one of the following categories according to Siskova et al. [27]: intact mitochondria with normal-appearing cristae (Type I); abnormal mitochondria with either swollen, irregular, or whirling cristae (Type II); mitochondria with discontinuous outer membrane or deficient cristae (Type III); mitochondria with both swollen and deficient cristae or both discontinuous outer membrane and swollen

cristae (Type IV). At least 14 mitochondria from each region were analysed for each animal.

Statistical data analysis

Group data are presented as the mean ± SEM. The statistical significance of between-group differences was assessed by a Tukey–Kramer test, Dunnett's test, or the paired t-test, using JMP software (SUS Institute, North Carolina, United States).

Result

Hetero-knockout of RP58 induced the early accumulation of DNA damage, activation of microglia, and ultrastructural changes in the mitochondria of neurons within the dentate gyrus during aging.

Figure 1B indicates that RP58 is highly expressed in mossy cells and granule cells in the dentate gyrus of the hippocampus in adults. Figure 1C and 1D illustrate the effect of RP58 hetero-knockout on DNA damage and repair. In the *RP58*$^{+/-}$ mice at 4-5 months, the accumulation of ssDNA and gamma-H2AX, which is a reporter of DNA double-strand breaks, in neurons within the dentate gyrus was detected. On the other hand, obvious accumulation of ssDNA and gamma-H2AX was not detected in the *RP58*$^{+/+}$ mice at 4-5 months. At 12-18 months, the accumulation of ssDNA and gamma-H2AX were detected in both genotypes. These results suggest that RP58 is involved in DNA damage and/or DNA repair in neurons within the dentate gyrus during the aging process. Figure 1E shows the effect of RP58 hetero-knockout on the activation of microglia, which has a strong relationship with DNA damage. In the *RP58*$^{+/-}$ mice at 4-5 months, activation of microglia within the dentate gyrus was significantly increased. At 12-18 months, obvious activation of microglia was detected in both genotypes. Although neuronal mitochondria are considered ‘immunometabolic hubs’ involved in

antigen presentation and the regulation of innate immune responses [3], we investigated the effect of RP58 hetero-knockout on neuronal mitochondria (Figure 1F). Mitochondria with both normal and abnormal ultrastructural appearance were present in each genotype, and we categorised them into four types, as indicated in the Materials and Methods section. The proportion of mitochondria by type in *RP58*$^{+/-}$ mice was different from that in *RP58*$^{+/+}$ mice. Furthermore, in the dentate gyrus of *RP58*$^{+/-}$ mice, mitochondria with swollen and deficient cristae, or swollen cristae and discontinuous outer membrane (Type IV), were detected. These results suggest that RP58 is involved in neuronal DNA damage.

Hetero-knockout of RP58 induced early impairment of cognitive function during aging.

Figure 2A illustrates the effect of hetero-knockout of RP58 on performance in the object location test, which evaluates spatial memory [6]. Object location memory in both genotypes was not altered at 2 months, as indicated by the fact that the discrimination index did not change. In contrast, object location memory in the *RP58*$^{+/-}$ mice at 4-5 months was impaired, as indicated by a discrimination index close to zero. Both *RP58*$^{+/-}$ mice and *RP58*$^{+/+}$ mice showed impaired object location memory at 12-18 months. These results indicate that hetero-knockout of RP58 influences object location

memory. Figure 2B shows the effect of RP58 hetero-knockout on theta power in the hippocampal CA1 region, which is crucial for spatial learning. In *RP58*$^{+/+}$ mice at 4-5 months, increased levels of theta power around the time of contact with objects on day 2 were revealed. However, this change in theta power n was not observed in *RP58*$^{+/-}$ mice at 4-5 months. These results suggested that hetero-knockout of RP58 induced deficits in learning ability.

Hetero-knockout of RP58 impaired the process of DNA repair.

Figure 3B and 3C illustrate the effect of the hetero-knockout of RP58 on DNA damage and repair. The expression of ssDNA within the dentate gyrus of both genotypes was revealed at 1 hour after the exposure to radiation. On the other hand, at 24 hours after exposure to radiation, the expression of ssDNA remained only in *RP58*$^{+/-}$ mice. Furthermore, the expression of gamma-H2AX, which is related to DNA repair, also remained only in the *RP58*$^{+/-}$ mice at 24 hours after the exposure to radiation. Figure 3D shows the effect of microglial activation. In the *RP58*$^{+/-}$ mice at 24 hours after the exposure to radiation, the microglia within the dentate gyrus remained activated. These results suggest that RP58 is involved in DNA repair.

Treatment with minocycline prevents for the early accumulation of DNA damage, activation of microglia, and impairment of cognitive function by hetero-knockout of RP58.

Figure 4B and 4C illustrate the effect of minocycline, which has neuroprotective and anti-inflammatory effects, for the early accumulation of DNA damage by hetero-knockout of RP58. Treatment with minocycline prevented the expression of ssDNA and gamma-H2AX at 4-5 months in *RP58*$^{+/-}$ mice. Figure 4D shows the effect of minocycline on the early activation of microglia by the hetero-knockout of RP58. Treatment with minocycline prevented the activation of microglia at 4-5 months in *RP58*$^{+/-}$ mice. Figure 4E shows the effect of minocycline on the impairment of object location memory. Treatment with minocycline prevented impairment at 4-5 months in *RP58*$^{+/-}$ mice. These results suggest that RP58 is involved in inflammation and DNA damage repair.

Discussion

We focused on the function of RP58 in DNA damage and repair, the mechanism of which, especially pertaining to aging, is currently unknown. We investigated whether RP58 plays an important role in the maintenance of cognitive function as an age-related phenomenon and the underlying mechanism. We found that the accumulation of DNA damage occurred early in the dentate gyrus of RP58 hetero-knockout mice. Since the hippocampus, including the dentate gyrus, plays a role in encoding spatial information, we performed an object location test to calculate spatial memory. We clarified that the impairment of spatial memory was detected early in RP58 hetero-knockout mice. At the stage of learning on day 2, an increase in theta power at the time of learning in the CA1 of RP58 hetero-knockout mice was weaker than that in the CA of wild-type mice. Therefore, RP58 hetero-knockout mice may not learn spatial information. Furthermore, the accumulation of DNA damage, abnormal activation of microglia, and impairment of spatial memory were prevented by treatment with minocycline, which has neuroprotective and anti-inflammatory effects.

The increase in DNMT3 expression, which is a co-repressor of RP58, was detected as an age-related change. It has been demonstrated that DNMT3 mutant cells fail to initiate DNA damage response. This phenomenon indicates impairment of DNA damage repair

[8]. However, it is unclear whether RP58 is related to DNA damage and repair. In the present study, we present the first evidence that RP58 is involved in DNA repair. Although there is a lack of detail, treatment with minocycline prevents the accumulation of DNA damage. Therefore, RP58 may play a role in autophagy in the DNA repair response, which is a point of application of minocycline. In fact, RND2, which receives inhibitory regulation by RP58[9], inhibits autophagy and apoptosis [30]. A decrease in autophagic activity is known as an age-related phenomenon and one of the causes of the accumulation of DNA damage [4]. Therefore, research on RP58 is important for determining the mechanism of aging.

Dysfunction of microglia, which plays a role in immune function, is an age-related change. Microglia change from a ramified morphological state to de-ramified, spheroid formation with abnormal processes in accordance with aging [14]. In the present study, microglial activation was detected in wild-type mice at 12-18 months. In contrast, in *RP58*$^{+/-}$ mice, microglial activation was detected at 4-5 months. Although microglia act protectively through inflammatory response and phagocytosis at an early stage, it has an injurious effect at the late stage. Given that minocycline, which selectively inhibits the activation of injurious microglia [13], prevents the activation of microglia in *RP58*$^{+/-}$ mice at 4-5 months, it is thought that microglia in *RP58*$^{+/-}$ mice at 4-5 months have

injurious properties. As pro-inflammatory microglia impair neurons [11], it cannot be ruled out that microglia may play a crucial role in the accumulation of DNA damage in *RP58*$^{+/-}$ mice.

It is thought that mitochondria in neurons are 'immunometabolic hubs', which relates with antigen presentation and innate immune reaction [3]. It has been demonstrated that the dysfunction of mitochondria is induced by metabolic imbalance, oxidative stress, inflammation, cellular injury or cell death in many pathologies [12, 27]. Abnormalities in mitochondria have been shown to be age-related changes [19]. The abnormality of mitochondria in neurons in *RP58*$^{+/-}$ mice, as observed in our study, may be caused by an abnormality in the immune system and DNA damage. RND2, which in under inhibitory regulation of RP58, binds and dephosphorylates p38, and inhibits autophagy. Therefore, a deficit in RP58 may induce the impairment of autophagy, resulting in the accumulation of abnormal mitochondria and toxic proteins (Figure 5)[29].

In the present study, DNA damage accumulation was detected in the dentate gyrus of *RP58*$^{+/-}$ mice. The hippocampus, including the dentate gyrus, plays a role in cognitive function [26]. We focused on the ability to define what is familiar and what is novel in the environment, and we observed an impairment of object location memory in *RP58*$^{+/-}$ mice at 4-5 months. In the LFP recording from the CA1, which is the output region of

the hippocampus, the enhancement of theta power, which were detected at the time of learning, in *RP58*$^{+/-}$ mice at the time of learning on days 2 and 3 were weaker than that in wild-type mice. Therefore, *RP58*$^{+/-}$ mice may not learn object location on day 2.

Considering our research and previous studies, *RP58*$^{+/-}$ mice may show dysfunction of the hippocampal network caused by the accumulation of DNA damage. To clarify the cause of the accumulation of DNA damage, we investigated whether the problem is in the DNA damage pathway or the DNA repair pathway using irradiation. Consequently, the accumulation of DNA damage in the dentate gyrus of *RP58*$^{+/-}$ mice was maintained at 24 hours after irradiation, despite similarity of DNA damage peak value in both genotypes. Therefore, it is assumed that RP58 plays a role in DNA repair, especially in autophagy.

In the present study, minocycline, which has neuroprotective and anti-inflammatory effects, prevented the accumulation of DNA damage, activation of microglia, and impairment of spatial memory. Minocycline has direct effects on DNA damage and on microglia. Additionally, it has indirect effects because of the relationship between DNA damage and inflammation [15, 25]. It is to be noted that we can not claim relationship, such as which is upstream, between DNA damage and inflammation. In the future, it is important to investigate neuronal network levels, including neurons, glia cells and other

factors.

In the present study, we established that RP58 plays a role in the accumulation of DNA damage and dysfunction of the immune system during aging. We advocated the importance of DNA repair pathway and the immune system through RP58 during aging.

Author contributions

T.T. and H.O. designed the research. T.T. performed and analyzed all experiments. K.E. performed sample preparation for electron microscopy. T.T. generated all the figures and tables and wrote the manuscript. H.O. edited the manuscript and supervised the study.

Acknowledgments

The authors thank Dr. Makoto Hashimoto for advice. The authors thank Kazuki Shiotani and Yuta Tanisumi for their contribution to help us with analysis of electrophysiology data. We would like to thank Editage (www.editage.com) for English language editing.

Funding

This work was partially supported by JSPS KAKENHI Grant Number 18H02537 for Haruo Okado, and by JSPS KAKENHI Grant Number 17K16408 and Research Grant for Public Health Science for Tomoko Tanaka.

Conflict of interest

The authors declare that the research was conducted in the absence of any commercial or financial relationships that could be construed as a potential conflict of interest.

Ethics approval

Approval was obtained from the Animal Experimentation Ethics Committee of the Tokyo Metropolitan Institute of Medical Science (49040).

1 Aoki K, Meng G, Suzuki K, Takashi T, Kameoka Y, Nakahara K, Ishida R, Kasai M (1998) RP58 associates with condensed chromatin and mediates a sequence-specific transcriptional repression. J Biol Chem 273: 26698-26704 Doi 10.1074/jbc.273.41.26698

2 Bachstetter AD, Van Eldik LJ, Schmitt FA, Neltner JH, Ighodaro ET, Webster SJ, Patel E, Abner EL, Kryscio RJ, Nelson PT (2015) Disease-related microglia heterogeneity in the hippocampus of Alzheimer's disease, dementia with Lewy bodies, and hippocampal sclerosis of aging. Acta Neuropathol Commun 3: 32

Doi 10.1186/s40478-015-0209-z
3 Bantug GR, Fischer M, Grählert J, Balmer ML, Unterstab G, Develioglu L, Steiner R, Zhang L, Costa ASH, Gubser PMet al (2018) Mitochondria-Endoplasmic Reticulum Contact Sites Function as Immunometabolic Hubs that Orchestrate the Rapid Recall Response of Memory CD8(+) T Cells. Immunity 48: 542-555.e546 Doi 10.1016/j.immuni.2018.02.012
4 Barbosa MC, Grosso RA, Fader CM (2018) Hallmarks of Aging: An Autophagic Perspective. Front Endocrinol (Lausanne) 9: 790 Doi 10.3389/fendo.2018.00790
5 Bialas AR, Presumey J, Das A, van der Poel CE, Lapchak PH, Mesin L, Victora G, Tsokos GC, Mawrin C, Herbst Ret al (2017) Microglia-dependent synapse loss in type I interferon-mediated lupus. Nature 546: 539-543 Doi 10.1038/nature22821
6 Denninger JK, Smith BM, Kirby ED (2018) Novel Object Recognition and Object Location Behavioral Testing in Mice on a Budget. J Vis Exp: Doi 10.3791/58593
7 Fuks F, Burgers WA, Godin N, Kasai M, Kouzarides T (2001) Dnmt3a binds deacetylases and is recruited by a sequence-specific repressor to silence transcription. Embo j 20: 2536-2544 Doi 10.1093/emboj/20.10.2536
8 Guryanova OA, Shank K, Spitzer B, Luciani L, Koche RP, Garrett-Bakelman FE, Ganzel C, Durham BH, Mohanty A, Hoermann Get al (2016) DNMT3A mutations promote anthracycline resistance in acute myeloid leukemia via impaired nucleosome remodeling. Nat Med 22: 1488-1495 Doi 10.1038/nm.4210
9 Heng JI, Qu Z, Ohtaka-Maruyama C, Okado H, Kasai M, Castro D, Guillemot F, Tan SS (2015) The zinc finger transcription factor RP58 negatively regulates Rnd2 for the control of neuronal migration during cerebral cortical development. Cerebral cortex 25: 806-816 Doi 10.1093/cercor/bht277
10 Hoeijmakers JH (2009) DNA damage, aging, and cancer. N Engl J Med 361: 1475-1485 Doi 10.1056/NEJMra0804615
11 Joshi AU, Minhas PS, Liddelow SA, Haileselassie B, Andreasson KI, Dorn GW, 2nd, Mochly-Rosen D (2019) Fragmented mitochondria released from microglia trigger A1 astrocytic response and propagate inflammatory neurodegeneration. Nat Neurosci 22: 1635-1648 Doi 10.1038/s41593-019-0486-0
12 Joshi AU, Mochly-Rosen D (2018) Mortal engines: Mitochondrial bioenergetics and dysfunction in neurodegenerative diseases. Pharmacological research 138:

2-15 Doi 10.1016/j.phrs.2018.08.010
13 Kobayashi K, Imagama S, Ohgomori T, Hirano K, Uchimura K, Sakamoto K, Hirakawa A, Takeuchi H, Suzumura A, Ishiguro Net al (2013) Minocycline selectively inhibits M1 polarization of microglia. Cell Death Dis 4: e525 Doi 10.1038/cddis.2013.54
14 Koellhoffer EC, McCullough LD, Ritzel RM (2017) Old Maids: Aging and Its Impact on Microglia Function. Int J Mol Sci 18: Doi 10.3390/ijms18040769
15 Li Y, Xie L, Huang T, Zhang Y, Zhou J, Qi B, Wang X, Chen Z, Li P (2019) Aging Neurovascular Unit and Potential Role of DNA Damage and Repair in Combating Vascular and Neurodegenerative Disorders. Front Neurosci 13: 778 Doi 10.3389/fnins.2019.00778
16 Lu H, Yue J, Meng X, Nickoloff JA, Shen Z (2007) BCCIP regulates homologous recombination by distinct domains and suppresses spontaneous DNA damage. Nucleic Acids Res 35: 7160-7170 Doi 10.1093/nar/gkm732
17 Lu T, Pan Y, Kao SY, Li C, Kohane I, Chan J, Yankner BA (2004) Gene regulation and DNA damage in the ageing human brain. Nature 429: 883-891 Doi 10.1038/nature02661
18 Maynard S, Fang EF, Scheibye-Knudsen M, Croteau DL, Bohr VA (2015) DNA damage, DNA repair, aging, and neurodegeneration. Cold Spring Harb Perspect Med 5: Doi 10.1101/cshperspect.a025130
19 Minhas PS, Latif-Hernandez A, McReynolds MR, Durairaj AS, Wang Q, Rubin A, Joshi AU, He JQ, Gauba E, Liu Let al (2021) Restoring metabolism of myeloid cells reverses cognitive decline in ageing. Nature 590: 122-128 Doi 10.1038/s41586-020-03160-0
20 Niraula A, Sheridan JF, Godbout JP (2017) Microglia Priming with Aging and Stress. Neuropsychopharmacology 42: 318-333 Doi 10.1038/npp.2016.185
21 Ohtaka-Maruyama C, Hirai S, Miwa A, Heng JI, Shitara H, Ishii R, Taya C, Kawano H, Kasai M, Nakajima Ket al (2013) RP58 regulates the multipolar-bipolar transition of newborn neurons in the developing cerebral cortex. Cell Rep 3: 458-471 Doi 10.1016/j.celrep.2013.01.012
22 Okado H (2019) Regulation of brain development and brain function by the transcriptional repressor RP58. Brain research 1705: 15-23 Doi 10.1016/j.brainres.2018.02.042
23 Okado H, Ohtaka-Maruyama C, Sugitani Y, Fukuda Y, Ishida R, Hirai S, Miwa A, Takahashi A, Aoki K, Mochida Ket al (2009) The transcriptional repressor RP58 is crucial for cell-division patterning and neuronal survival in the

developing cortex. Dev Biol 331: 140-151 Doi 10.1016/j.ydbio.2009.04.030
24 Perry VH, Holmes C (2014) Microglial priming in neurodegenerative disease. Nat Rev Neurol 10: 217-224 Doi 10.1038/nrneurol.2014.38
25 Raj DD, Jaarsma D, Holtman IR, Olah M, Ferreira FM, Schaafsma W, Brouwer N, Meijer MM, de Waard MC, van der Pluijm Iet al (2014) Priming of microglia in a DNA-repair deficient model of accelerated aging. Neurobiol Aging 35: 2147-2160 Doi 10.1016/j.neurobiolaging.2014.03.025
26 Scharfman HE (2016) The enigmatic mossy cell of the dentate gyrus. Nat Rev Neurosci 17: 562-575 Doi 10.1038/nrn.2016.87
27 Sisková Z, Mahad DJ, Pudney C, Campbell G, Cadogan M, Asuni A, O'Connor V, Perry VH (2010) Morphological and functional abnormalities in mitochondria associated with synaptic degeneration in prion disease. Am J Pathol 177: 1411-1421 Doi 10.2353/ajpath.2010.091037
28 Sisková Z, Page A, O'Connor V, Perry VH (2009) Degenerating synaptic boutons in prion disease: microglia activation without synaptic stripping. Am J Pathol 175: 1610-1621 Doi 10.2353/ajpath.2009.090372
29 Vessoni AT, Filippi-Chiela EC, Menck CF, Lenz G (2013) Autophagy and genomic integrity. Cell Death Differ 20: 1444-1454 Doi 10.1038/cdd.2013.103
30 Xu Y, Sun Q, Yuan F, Dong H, Zhang H, Geng R, Qi Y, Xiong X, Chen Q, Liu B (2020) RND2 attenuates apoptosis and autophagy in glioblastoma cells by targeting the p38 MAPK signalling pathway. J Exp Clin Cancer Res 39: 174 Doi 10.1186/s13046-020-01671-2
31 Zhang L, Huang P, Chen H, Tan W, Lu J, Liu W, Wang J, Zhang S, Zhu W, Cao Jet al (2017) The inhibitory effect of minocycline on radiation-induced neuronal apoptosis via AMPKα1 signaling-mediated autophagy. Sci Rep 7: 16373 Doi 10.1038/s41598-017-16693-8

Figure Legends

Figure.1 Hetero-knockout of RP58 induced the accumulation of DNA damage and the abnormality of neuronal mitochondria, and the activation of microglia.

(A) Experimental schedule during aging. (B) RP58 is highly expressed in mossy cells and granule cells in the dentate gyrus in adult. (C, D) The accumulation of DNA damage was detected by ssDNA (magenta) and gamma-H2AX (grey). Hetero-knockout of RP58 increases the accumulation of ssDNA within neurons (arrow) in the dentate gyrus of the hippocampus at 4-5 months. ***$p < 0.001$ $RP58^{+/+}$ mice at 2 months vs. $RP58^{+/-}$ mice at 4-5 months, ***$p < 0.001$ $RP58^{+/+}$ mice at 2 months vs. $RP58^{+/+}$ mice at 12-18 months, ***$p < 0.001$ $RP58^{+/+}$ mice at 2 months vs. $RP58^{+/-}$ mice at 12-18 months; n = 3 mice/ $RP58^{+/+}$ mice at 2 months, n = 3 mice/ $RP58^{+/-}$ mice at 2 months, n = 4 mice/ $RP58^{+/+}$ mice at 4-5 months, n = 4 mice/ $RP58^{+/-}$ mice at 4-5 months, n = 3 mice/ $RP58^{+/+}$ mice at 12-18 months, n = 3 mice/ $RP58^{+/-}$ mice at 12-18 months (Dunnett's test). Hetero-knockout of RP58 increases the accumulation of gamma-H2AX within neurons (arrow) in the dentate gyrus of the hippocampus at 4-5 months. *$p < 0.05$ $RP58^{+/+}$ mice at 2 months vs. $RP58^{+/-}$ mice at 4-5 months, *$p < 0.05$ $RP58^{+/+}$ mice at 2 months vs. $RP58^{+/+}$ mice at 12-18 months, **$p < 0.05$ $RP58^{+/+}$ mice at 2 months vs.

RP58$^{+/-}$ mice at 12-18 months; n = 3 mice/ RP58$^{+/+}$ mice at 2 months, n = 3 mice/ RP58$^{+/-}$ mice at 2 months, n = 4 mice/ RP58$^{+/+}$ mice at 4-5 months, n = 4 mice/ RP58$^{+/-}$ mice at 4-5 months, n = 3 mice/ RP58$^{+/+}$ mice at 12-18 months, n = 3 mice/ RP58$^{+/-}$ mice at 12-18 months (Dunnett's test) (E) Microglial activation was detected by labelling microglia with Iba1 (magenta) and labelling activation with CD68 (cyan). Hetero-knockout of RP58 activates microglia in the dentate gyrus of the hippocampus at 4-5 months. **$p < 0.01$ RP58$^{+/+}$ mice at 2 months vs RP58$^{+/-}$ mice at 4-5 months, *$p < 0.05$ RP58$^{+/+}$ mice at 2 months vs. RP58$^{+/+}$ mice at 12-18 months, **$p < 0.01$ RP58$^{+/+}$ mice at 2 months vs RP58$^{+/-}$ mice at 12-18 months; n = 3 mice/ RP58$^{+/+}$ mice at 2 months, n = 3 mice/ RP58$^{+/-}$ mice at 2 months, n = 4 mice/ RP58$^{+/+}$ mice at 4-5 months, n = 4 mice/ RP58$^{+/-}$ mice at 4-5 months, n = 3 mice/ RP58$^{+/+}$ mice at 12-18 months, n = 3 mice/ RP58$^{+/-}$ mice at 12-18 months (Dunnett's test) (F) For identification of neuronal mitochondria, the criteria of Siskova et al. were used. Every mitochondria of neuronal origin were analysed and based on their ultrastructural appearance, classified into one of four categories by Siskova et al. RP58$^{+/-}$ mice at 4-5 months had more mitochondria with abnormal ultrastructural appearance in the granule cell layer and hilus of the dentate gyrus in the hippocampus. Granule cell layer: Chai-square = 284.837, df = 3, p

< 0.001; Hilus: Chai-square = 359.525, df = 3, p < 0.001; n = 3 mice/each per group (Pearson's chi-squared test)

Figure. 2 Hetero-knockout of RP58 induces the impairment of spatial learning.

(A) Spatial memory was measured using an object location test. $RP58^{+/-}$ mice at 4-5 months showed the impairment of spatial memory. *p < 0.05 $RP58^{+/+}$ mice at 2 months vs $RP58^{+/-}$ mice at 4-5 months, **p < 0.01 $RP58^{+/+}$ mice at 2 months vs. $RP58^{+/+}$ mice at 12-18 months; n = 12 mice/ $RP58^{+/+}$ mice at 2 months, n = 12 mice/ $RP58^{+/-}$ mice at 2 months, n = 12 mice/ $RP58^{+/+}$ mice at 4-5 months, n = 12 mice/ $RP58^{+/-}$ mice at 4-5 months, n = 10 mice/ $RP58^{+/+}$ mice at 12-18 months, n = 16 mice/ $RP58^{+/-}$ mice at 12-18 months (Dunnett's test) (B) LFPs in CA1 of hippocampus were recorded during object location test on day 2 and day 3 at 4 months. Increase of theta powers in CA1 were detected around the time of contacting the object in $RP58^{+/+}$ mice at 4months on day 2 and day 3 compared to baseline. On the other hand, in $RP58^{+/-}$ mice at 4 months, theta power in CA1 were weaker than that in $RP58^{+/+}$ mice on day 2 and there is no significant change in theta power on day 3 compared to baseline. Day 2 Theta: # p < 0.05 vs $RP58^{+/+}$ mice baseline or $RP58^{+/-}$ mice baseline, *p < 0.05 $RP58^{+/+}$ mice vs $RP58^{+/-}$ mice. Day 3 Theta: # p < 0.05 vs $RP58^{+/+}$ mice baseline or $RP58^{+/-}$ mice

baseline,*$p < 0.05$ $RP58^{+/+}$ mice vs $RP58^{+/-}$ mice. n = 5 mice/each per group (Paired t-test, Turkey-Kramer test, Wilcoxon signed-rank test)

Figure.3 Hetero-knockout of RP58 impaired the ability of DNA repair.

(A) Sampling schedule after irradiation. (B, C) The accumulation of DNA damage was detected by ssDNA (magenta) and gamma-H2AX (grey). In $RP58^{+/-}$ mice at 2 months, the accumulation of ssDNA within neurons in the dentate gyrus of the hippocampus was sustained at 24 hours after irradiation. *$p < 0.05$ $RP58^{+/+}$ mice at 1hour after irradiation vs. $RP58^{+/+}$ mice at 24 hours after irradiation; n = 3/each per group (Dunnett's test). In $RP58^{+/-}$ mice at 2 months, the accumulation of gamma-H2AX within neurons in the dentate gyrus of the hippocampus was sustained at 24 hours after irradiation. **$p < 0.01$ $RP58^{+/+}$ mice at 1hour after irradiation vs. $RP58^{+/+}$ mice at 24 hours after irradiation; n = 3/each per group (Dunnett's test) (D) Microglial activation was detected by labelling microglia with Iba1 (magenta) and labelling activation with CD68 (cyan). In $RP58^{+/-}$ mice at 24 hours after irradiation, activated microglia were much more abundant than $RP58^{+/+}$ mice at 24 hours after irradiation. **$p < 0.01$ $RP58^{+/+}$ mice at 1hour after irradiation vs. $RP58^{+/+}$ mice at 24 hours after irradiation; n = 3/each per group (Dunnett's test)

Figure.4 The accumulation of DNA damage, the activation of microglia and the impairment of spatial memory by hetero-knockout of RP58 prevented by the treatment of minocycline.

(A) Experimental schedule of drug intervention. (B) The accumulation of ssDNA with in neuron in dentate gyrus of hippocampus at 4-5 months in $RP58^{+/-}$ mice prevented by the treatment of minocycline. *$p < 0.05$ $RP58^{+/+}$ mice at 4-5 months vs. $RP58^{+/-}$ mice at 4-5 months; n = 3/each per group (Dunnett's test) (C) The accumulation of gamma-H2AX with in neuron in dentate gyrus of hippocampus at 4-5 months in $RP58^{+/-}$ mice prevented by the treatment of minocycline. *$p < 0.05$ $RP58^{+/+}$ mice at 4-5 months vs. $RP58^{+/-}$ mice at 4-5 months; n = 3/each per group (Dunnett's test) (D) The activation of microglia in dentate gyrus of hippocampus in $RP58^{+/-}$ mice at 4-5 months prevented by the treatment of minocycline. *$p < 0.05$ $RP58^{+/+}$ mice at 4-5 months vs. $RP58^{+/-}$ mice at 4-5 months; n = 3/each per group (Dunnett's test) (E) The impairment of spatial memory in $RP58^{+/-}$ mice at 4-5 months prevented by the treatment of minocycline. $p = 0.0646$ $RP58^{+/+}$ mice at 4-5 months vs. $RP58^{+/-}$ mice at 4-5 months; n = 12 mice/ $RP58^{+/+}$ mice at 4-5 months, n = 12 mice/ $RP58^{+/-}$ mice at 4-5 months, n = 9 mice/ $RP58^{+/+}$ mice with minocycline at 4-5 months, n = 13 mice/ $RP58^{+/-}$ mice with minocycline at 4-5 months (Dunnett's test)

Figure. 5 Mechanistic model for RP58 regulation of DNA damage accumulation and microglial activation

(A)

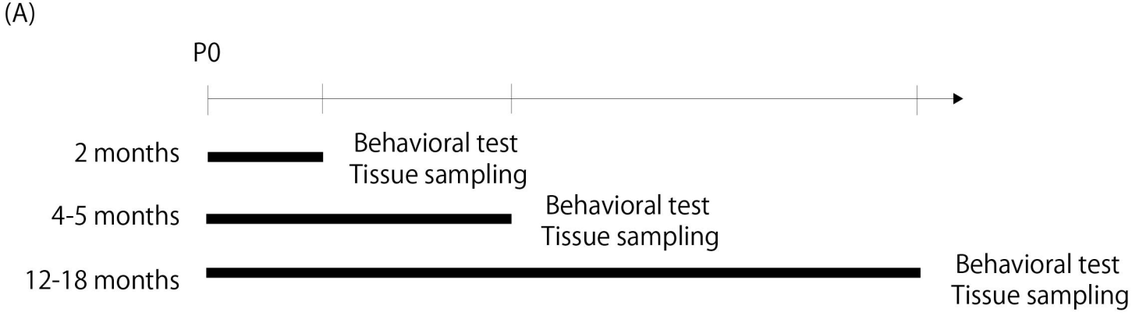

(B)

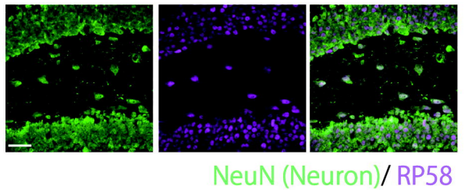

(C)

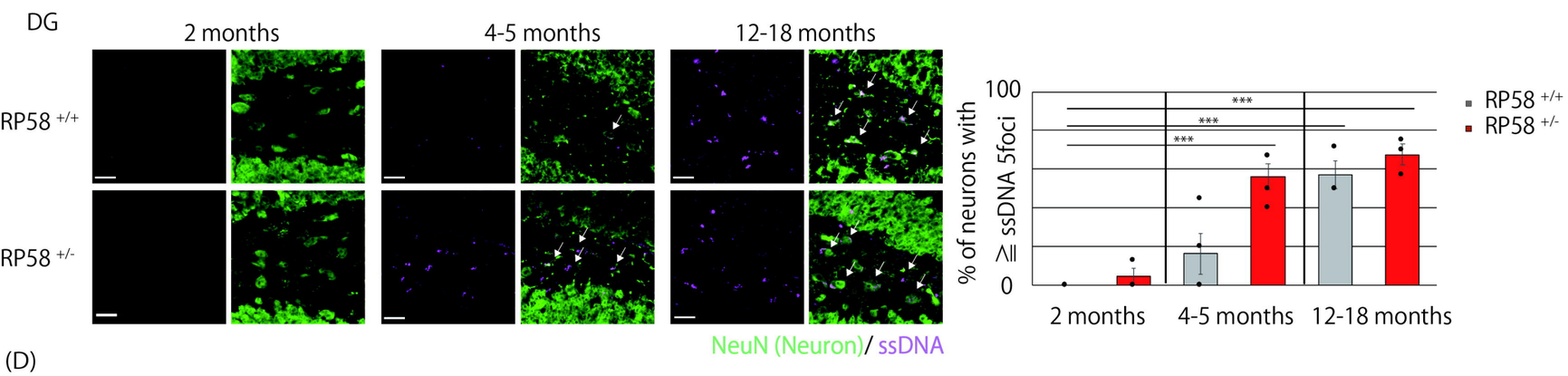

(D)

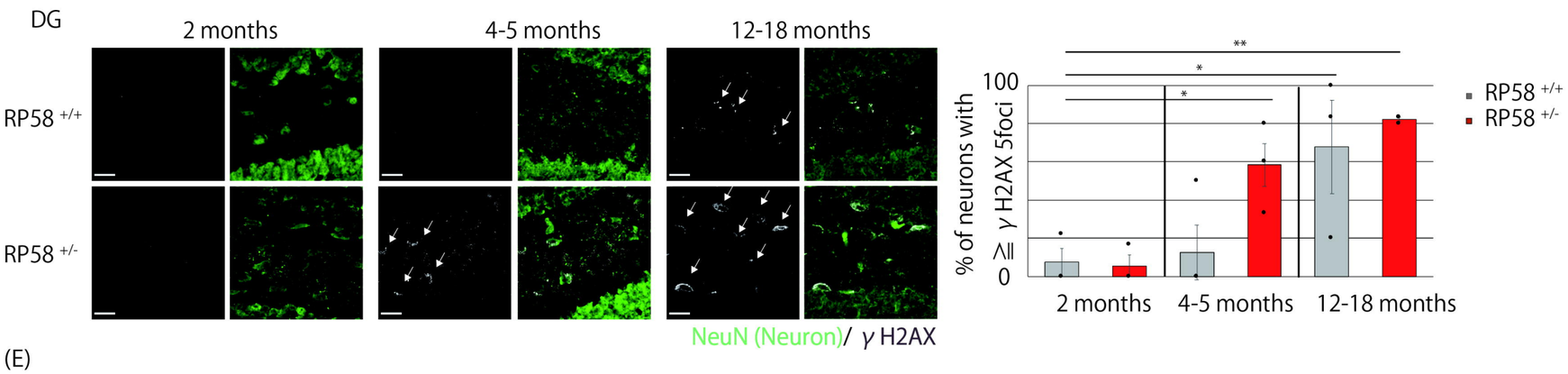

(E)

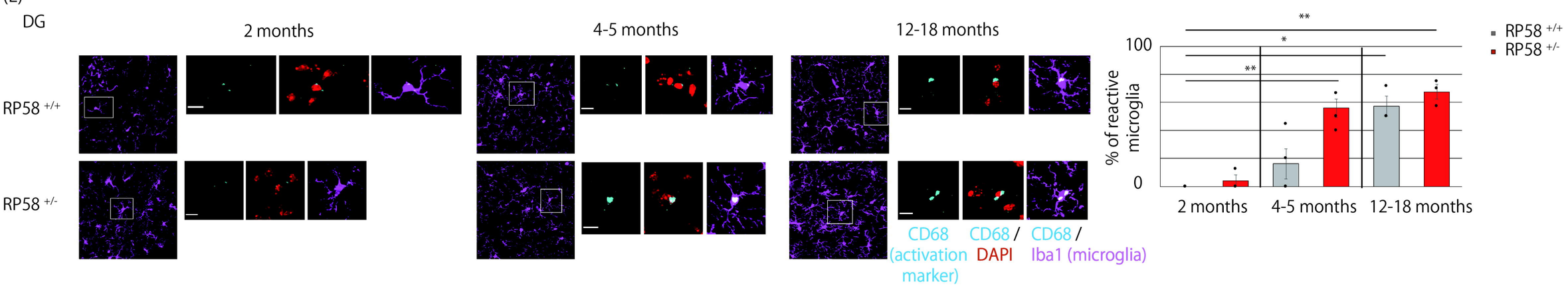

(F) 4-5 months

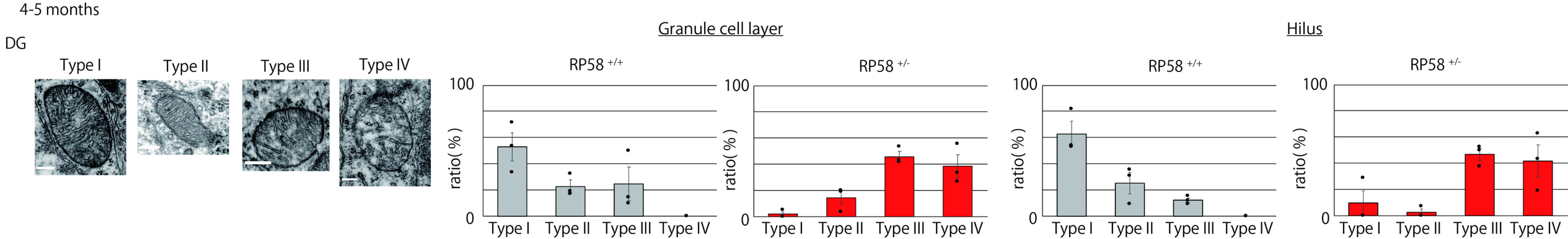

(A)

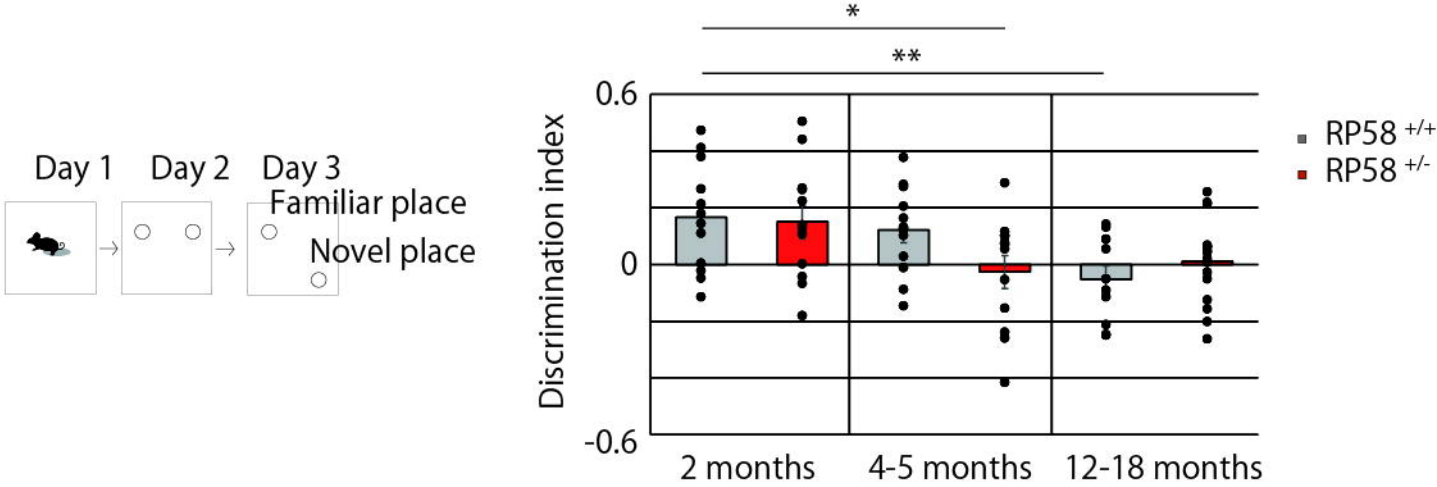
Day 1
Day 2
Day 3
Familiar place
Novel place
*
**
0.6
0
-0.6
Discrimination index
2 months
4-5 months
12-18 months
RP58 +/+
RP58 +/-

(B)

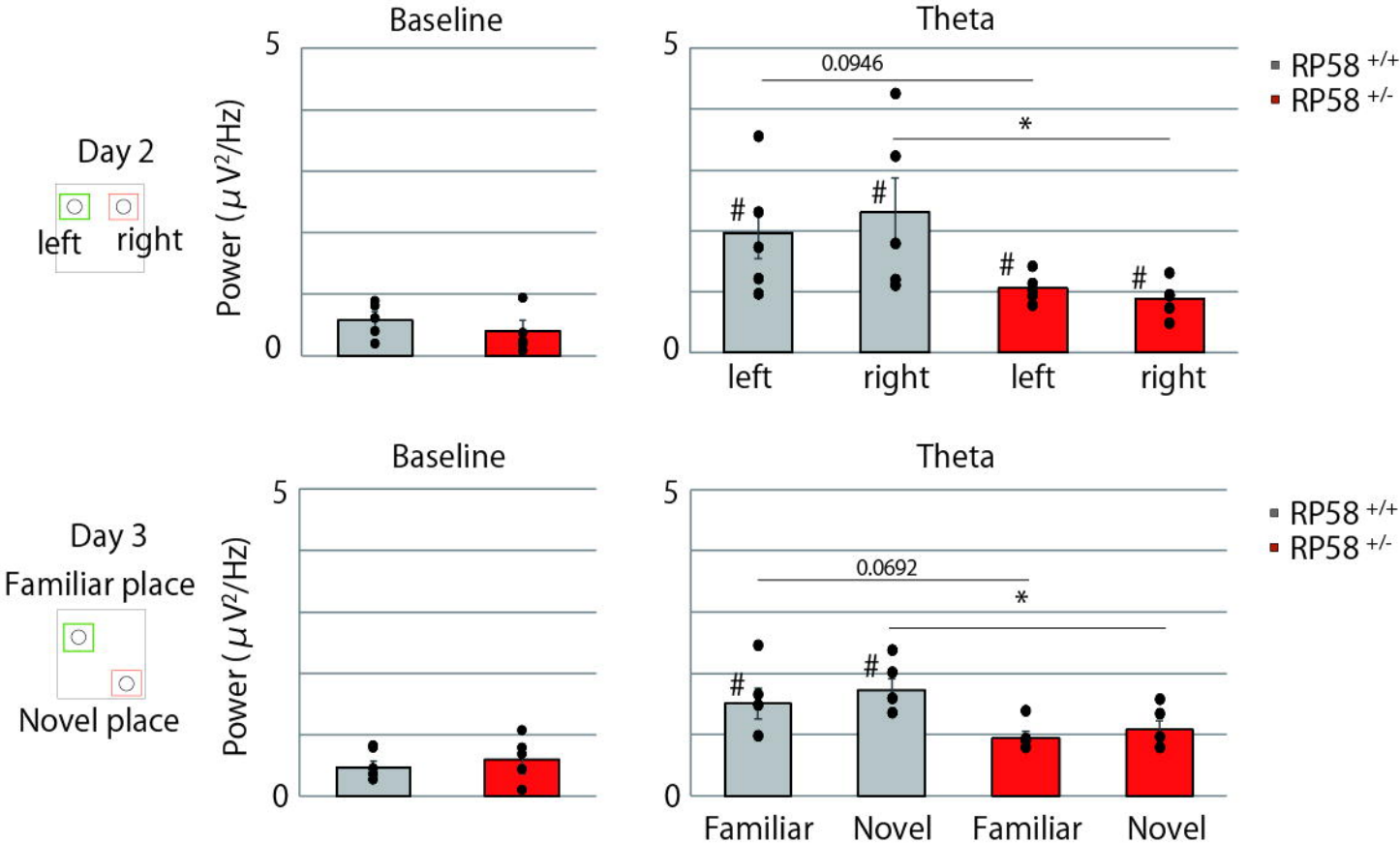
Day 2
left
right
Baseline
Theta
5
0
Power (μ V²/Hz)
0.0946
*
#
left
right
left
right
RP58 +/+
RP58 +/-
Day 3
Familiar place
Novel place
0.0692
Familiar
Novel
Familiar
Novel

(A)

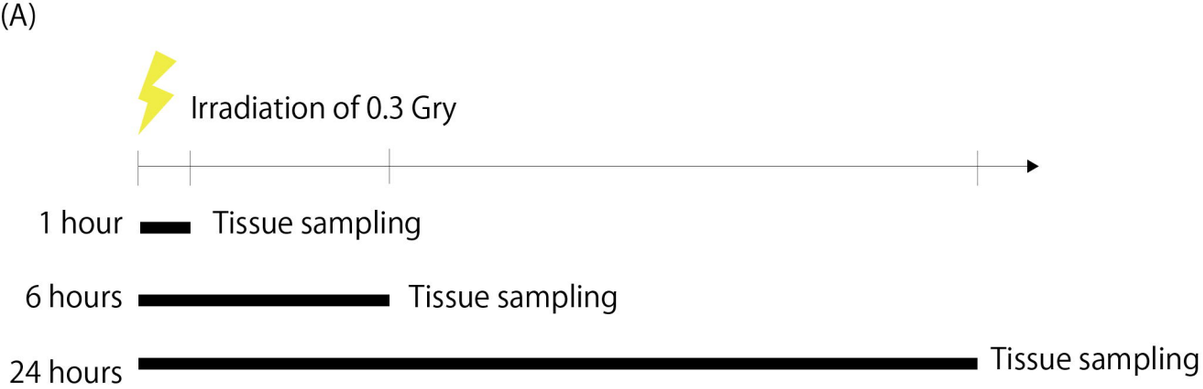
Irradiation of 0.3 Gry
1 hour
Tissue sampling
6 hours
Tissue sampling
24 hours
Tissue sampling

(B)

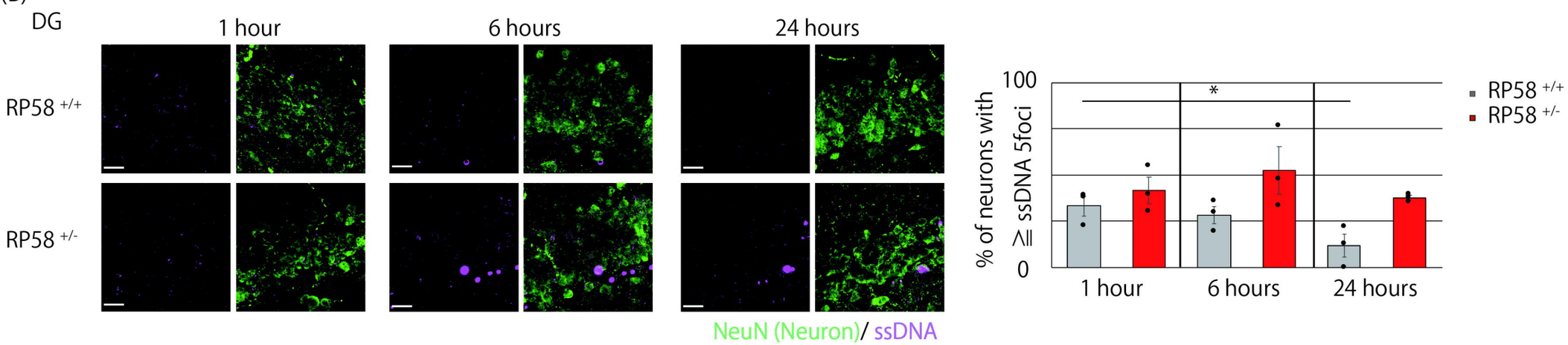
DG
1 hour
6 hours
24 hours
RP58 +/+
RP58 +/-
NeuN (Neuron)/ ssDNA
% of neurons with ≧ ssDNA 5foci
100
0
*
1 hour
6 hours
24 hours
RP58 +/+
RP58 +/-

(C)

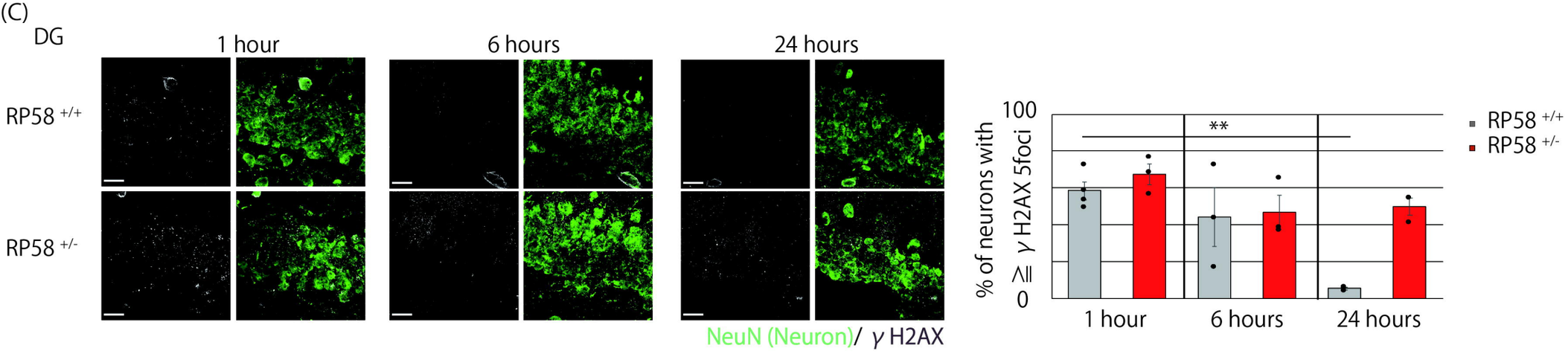
DG
1 hour
6 hours
24 hours
RP58 +/+
RP58 +/-
NeuN (Neuron)/ γ H2AX
% of neurons with ≧ γ H2AX 5foci
100
0
**
1 hour
6 hours
24 hours
RP58 +/+
RP58 +/-

(D)

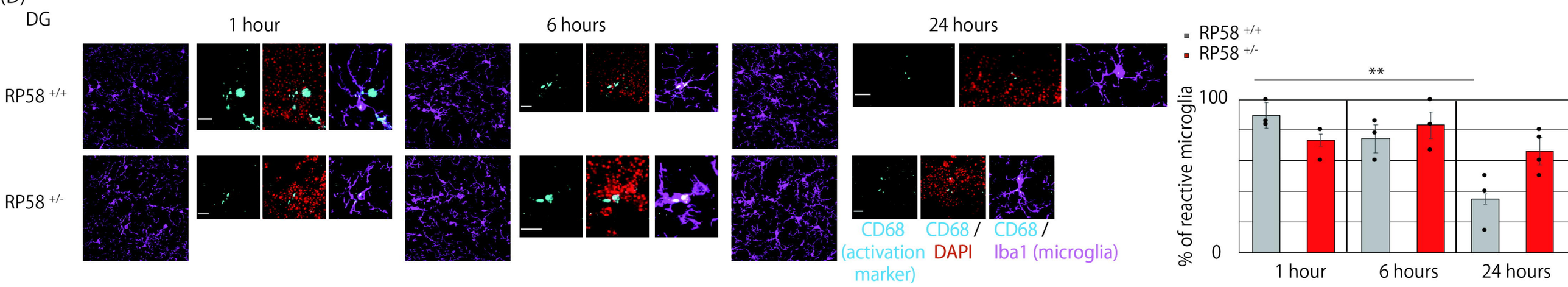
DG
1 hour
6 hours
24 hours
RP58 +/+
RP58 +/-
CD68 (activation marker)
CD68 / DAPI
CD68 / Iba1 (microglia)
RP58 +/+
RP58 +/-
**
% of reactive microglia
100
0
1 hour
6 hours
24 hours

(A)

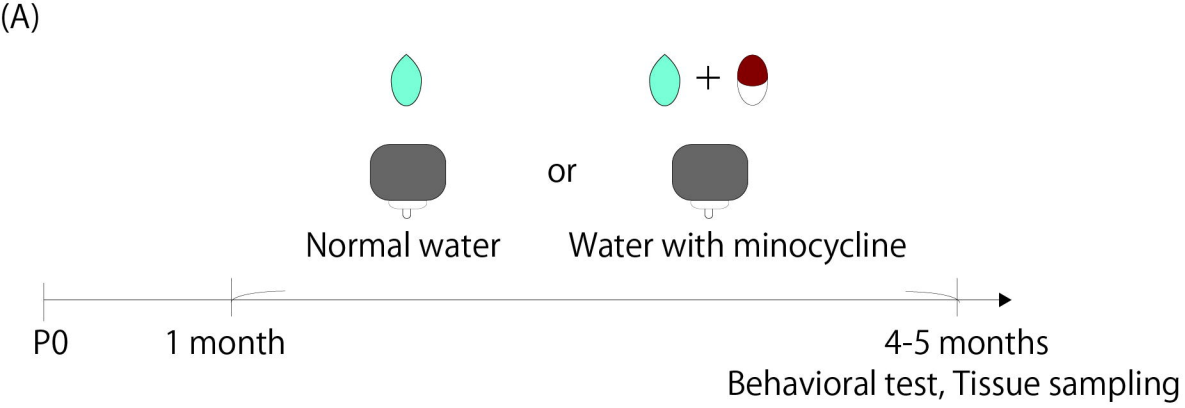
or
Normal water
Water with minocycline
P0
1 month
4-5 months
Behavioral test, Tissue sampling

(B)

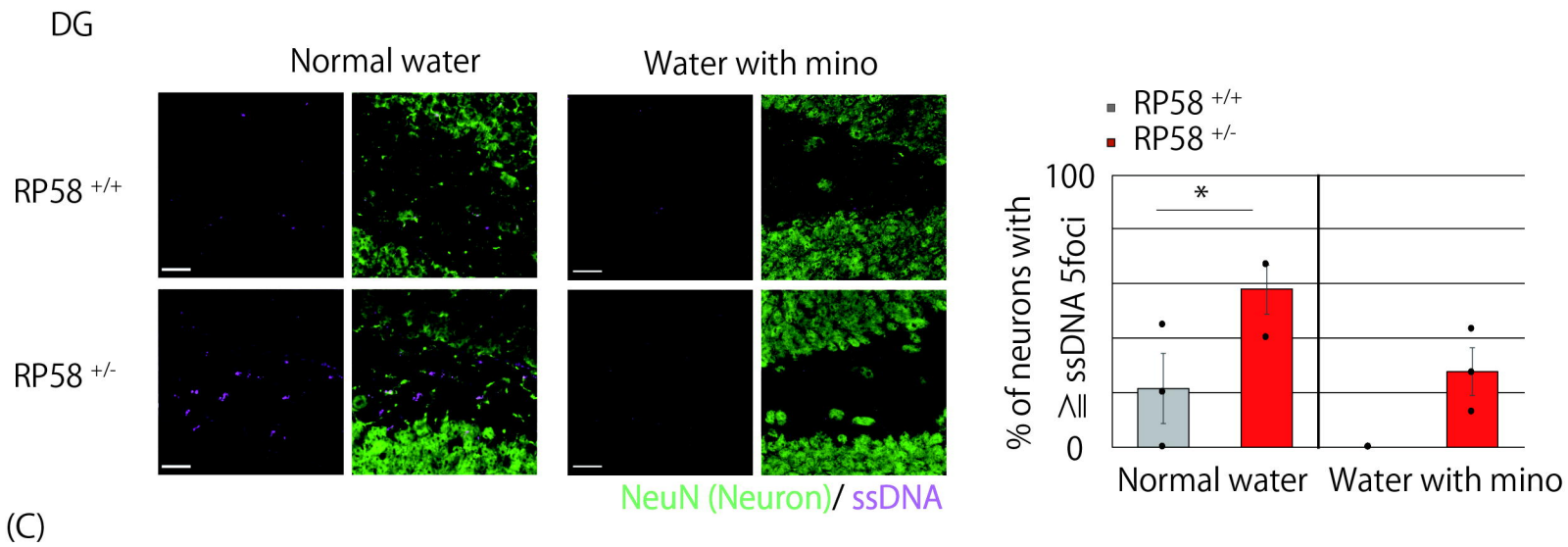
DG
Normal water
Water with mino
RP58 +/+
RP58 +/-
NeuN (Neuron)/ ssDNA
RP58 +/+
RP58 +/-
% of neurons with ≧ ssDNA 5foci
100
0
*
Normal water
Water with mino

(C)

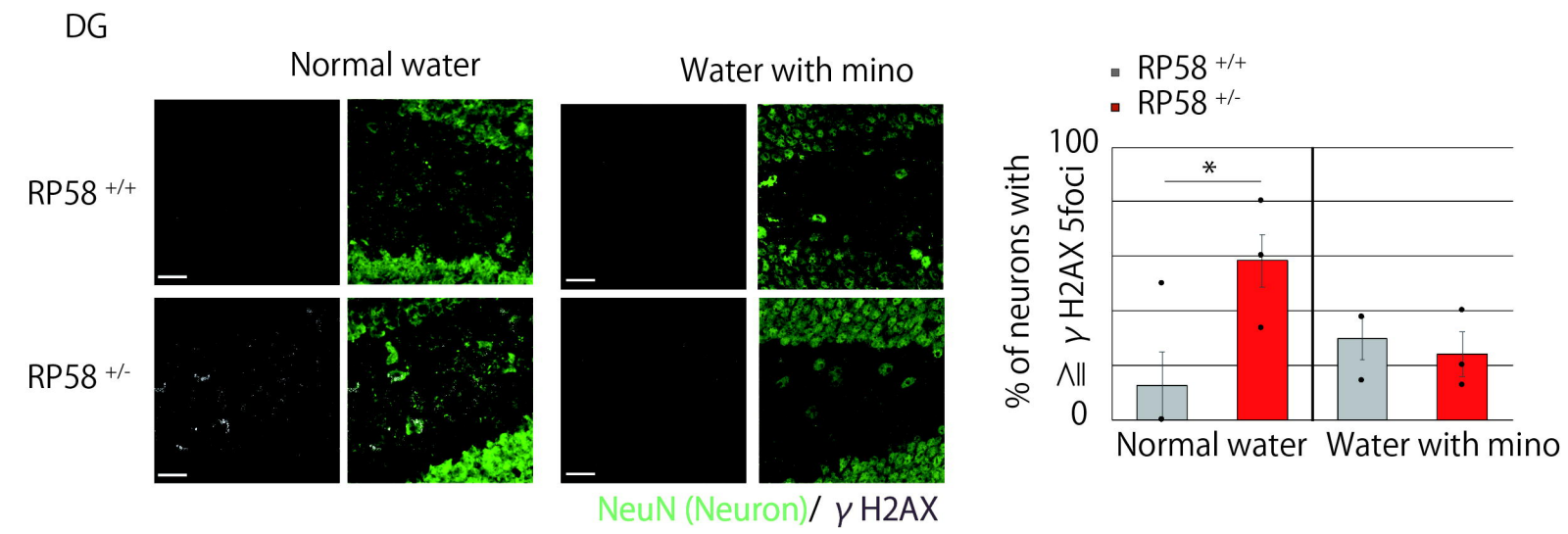
DG
Normal water
Water with mino
RP58 +/+
RP58 +/-
NeuN (Neuron)/ γ H2AX
RP58 +/+
RP58 +/-
% of neurons with ≧ γ H2AX 5foci
100
0
*
Normal water
Water with mino

(D)

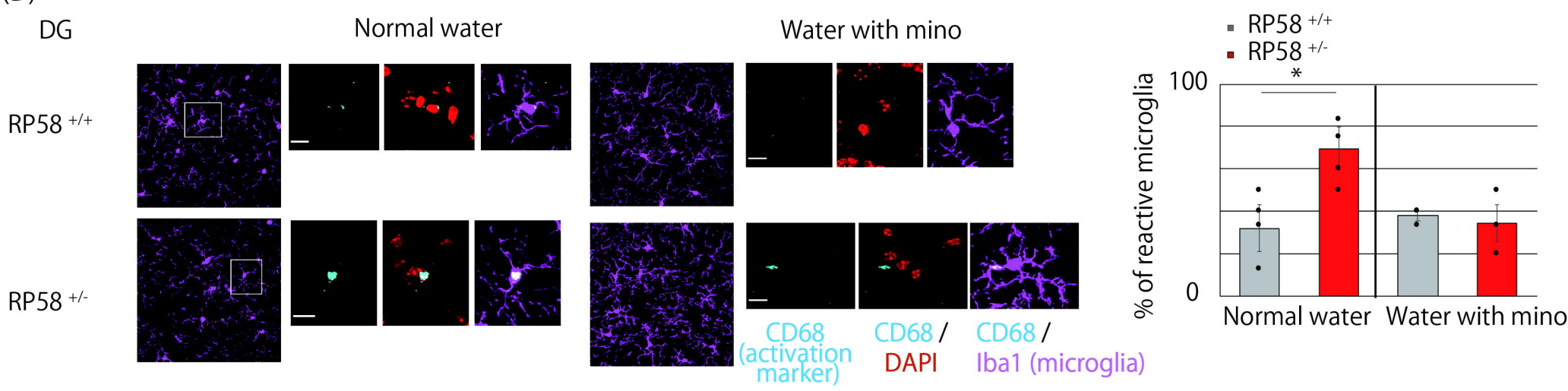
DG
Normal water
Water with mino
RP58 +/+
RP58 +/-
CD68 (activation marker)
CD68 / DAPI
CD68 / Iba1 (microglia)
RP58 +/+
RP58 +/-
% of reactive microglia
100
0
*
Normal water
Water with mino

(E)

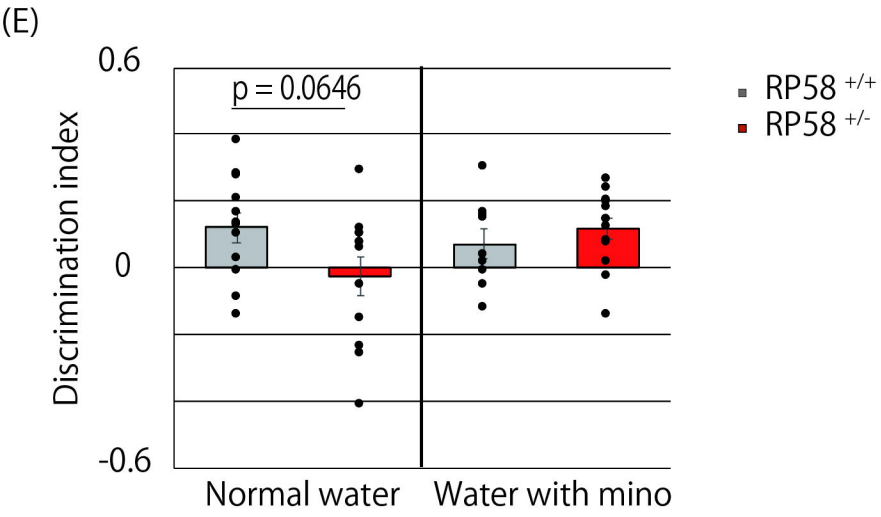
Discrimination index
0.6
0
-0.6
p = 0.0646
RP58 +/+
RP58 +/-
Normal water
Water with mino

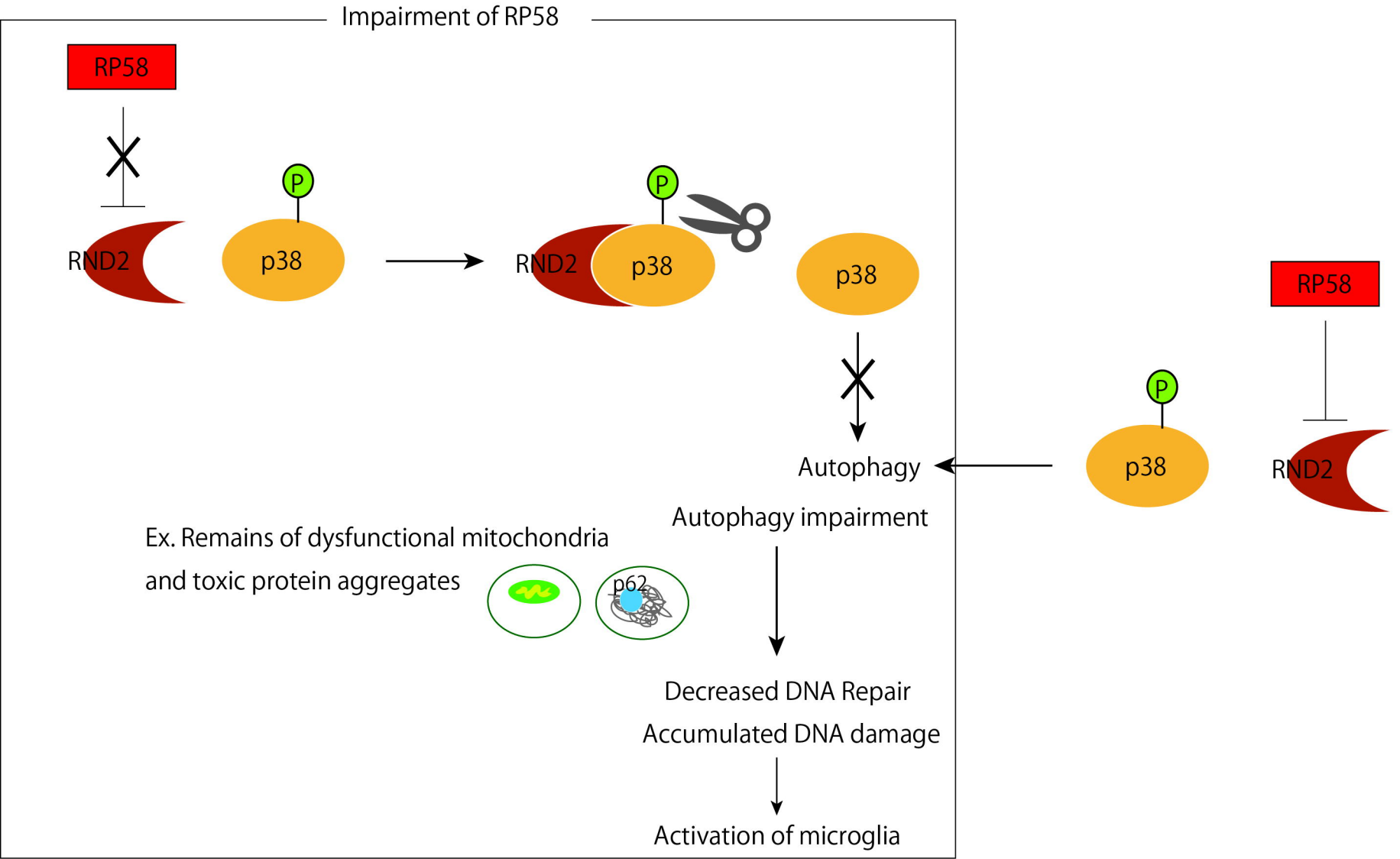
Impairment of RP58
RP58
RND2
P
p38
RND2
P
p38
p38
Autophagy
Autophagy impairment
Ex. Remains of dysfunctional mitochondria
and toxic protein aggregates
p62
Decreased DNA Repair
Accumulated DNA damage
Activation of microglia
P
p38
RP58
RND2

Primary antibody
Mouse anti-NeuN (Merck., Darmstadt, Germany)
Chicken anti-RP58 (Takahashi et al., 2008)
Rabbit anti-ssDNA (IBL., Gunma, Japan)
Rabbit anti-gamma H2AX (Abcam., Cambridge, United Kingdom)
Rabbit anti-Iba1 (FUJIFILM., Tokyo, Japan)
Rat anti-CD68 (Abcam., Cambridge, United Kingdom)